JTTEE5 14:369-372
DOI: 10.1361/105996305X59440
1059-9630/$19.00 © ASM International

Effect of High-Velocity Oxygen-Fuel Thermal Spraying on the Physical and Mechanical Properties of Type 316 Stainless Steel

T.C. Totemeier

(Submitted December 8, 2003; in revised form February 24, 2004)

Data on the microstructural, physical, and mechanical characteristics of high-velocity oxygen-fuel (HVOF)-sprayed type 316 stainless steel coatings are presented and compared with properties of wrought 316 stainless steel. Coatings were prepared at three different spray particle velocities; coating characteristics are presented as a function of velocity. The coatings had relatively low porosity and oxide contents and were significantly harder than annealed, wrought 316 stainless steel. The hardness difference is primarily attributed to high dislocation densities resulting from peening imparted by high-velocity spray particles. The coating hardness increased with increasing spray particle velocity, reflecting increased peening effects. The elastic modulus of the coatings was essentially identical to wrought material. The mean coefficient of thermal expansion of as-sprayed coatings was lower than wrought material, but the expansion of annealed coatings matched the wrought behavior.

Keywords coatings, hardness, high-velocity oxygen-fuel, stainless steel, thermal expansion, thermal spray

1. Introduction

Thermally sprayed coatings are increasingly used in applications requiring wear and high-temperature oxidation resistance. Various analytical and numerical models have been developed to predict the development of stresses during deposition and in service (Ref 1-4). Knowledge of the physical and microstructural characteristics of the coating and substrate is crucial in successful model implementation. Experience has shown that coating properties, for example, elastic modulus, can be markedly different than those of nominally identical bulk materials, and considerable effort has been made to measure actual coating properties (Ref 5-10). Study of coating mechanical and physical properties to date appears to have somewhat favored plasma-sprayed ceramic coatings because these are used widely as thermal barriers in gas turbine engines and have properties that are very different than bulk ceramics.

Although many papers describe the microstructure and hardness of high-velocity oxygen-fuel (HVOF) coatings exist (Ref 11-14), fewer report other mechanical and physical characteristics such as elastic modulus and thermal expansion coefficient (Ref 15, 16). This is likely a result of the difficulty in making unambiguous measurements of these properties, but perhaps also the result of an incorrect assumption that the properties of HVOF coatings (especially metallic coatings) are essentially identical to cast or wrought alloys of equivalent composition because of their typically low oxide and porosity contents. In recent measurements on Fe_3Al intermetallic coatings formed by HVOF spraying, however, some significant differences were observed compared with typical wrought alloys, particularly for hardness and thermal expansion coefficient (Ref 17). Clear interpretation of the data was difficult because of ordering transformations that occur in these intermetallic alloys.

This paper presents data on the microstructural, physical, and mechanical characteristics of HVOF-sprayed type 316L stainless steel (SS) coatings. This alloy is appropriate for study because of its single-phase structure and potential use as a corrosion-resistant surface layer. It is expected to typify the behavior of a number of austenitic, solid-solution-strengthened alloys. Coatings of this alloy will also be used in a study of residual stresses calculated from curvature of coating-substrate couples; precise coating data are required for modeling.

2. Coating Preparation and Characterization

A JP5000 HVOF spray gun (Praxair-Tafa, Concord, NH) with a 0.10 m barrel was used to prepare coatings from gas-atomized AISI type 316L SS feedstock powder (Tafa, 1235F) at a fixed standoff distance of 0.355 m. The powder was screened to –270 mesh prior to spraying; 94% of the powder was in the 20-38 μm size range, with 4% between 38 and 45 μm. Essentially no particles were smaller than 20 μm. The coatings were built up layer by layer using a raster deposition scheme; each pass in front of the torch at a transverse velocity of 0.20 m/s produced an approximately 45 μm thick layer.

Coatings were applied to 6.4 mm thick type 316 SS substrates that were grit blasted on both sides with alumina prior to spraying; total coating thicknesses were approximately 1500 μm, permitting production of freestanding specimens for modulus and thermal expansion measurements. Coatings were produced

T.C. Totemeier, Idaho National Laboratory, Idaho Falls, ID 83415. Contact e-mail: terry-totemeier@inl.gov.

Table 1 HVOF spray conditions and particle characteristics

Oxygen flow(a), L/min	Kerosene flow, L/h	Chamber gauge pressure, kPa	Mean spray particle temperature (b), °C	Spray particle velocity	
				Mean, m/s	Standard deviation, m/s
520	16.7	350	1320	520	36
700	22.7	510	1310	610	44
820	26.5	614	1300	640	46

(a) At standard temperature and pressure. (b) The temperature sensor does not discriminate individual particles, hence the distribution of particle temperatures is unavailable.

at an equivalence ratio of 1 (a stoichiometric mixture of kerosene and oxygen) and three torch chamber gauge pressures, 170, 340, and 620 kPa. The particle temperature and velocity characteristics for each condition were measured using an integrated laser Doppler velocimeter and high-speed two-color pyrometer. The estimated, 1σ, measurement uncertainties are 5% for particle temperature (assuming gray body behavior) and less than 5 m/s for particle velocity (Ref 18, 19). Table 1 lists details of the spray conditions and resulting particle characteristics.

Coating microstructures were characterized by standard metallographic techniques. Coating-substrate couples were sectioned using a low-speed diamond saw, hot mounted in a thermal setting resin, ground, and polished to a 1 μm finish. The volume fractions of porosity, oxide, and unmelted particles were measured by image analysis of representative microstructures obtained using secondary and backscattered electron imaging. The error in the values obtained is estimated to be 20% of the value. X-ray line broadening analysis (described in Ref 20) was used to measure the coherently diffracting domain size (subgrain size) and the root mean square lattice microstrain of the coatings and the feedstock powder. These two parameters were converted to an equivalent dislocation density (Ref 21). Vickers pyramidal microhardness was measured with a 500 g load, and Rockwell C-hardness measurements were made on polished coating surfaces.

Elastic moduli were measured on freestanding, rectangular coatings (dimensions 20 × 10 × 1 mm) elastically loaded in compression. The freestanding coatings were prepared by careful sectioning of coating-substrate couples using a low-speed diamond saw followed by grinding on 600 grit SiC paper. Small strain gages were attached to the specimens using epoxy. The mean thermal expansion coefficient (CTE) was measured on freestanding coatings using a Theta Industries (Port Washington, NY) vertical dilatometer operating in differential mode; a Pt standard was used as the reference. The specimens were heated at 3 °C/min in a rough vacuum; low contact forces were used to minimize creep deformation at high temperatures. Three sequential runs were performed on each specimen to observe changes in expansion behavior with annealing and thermal cycling.

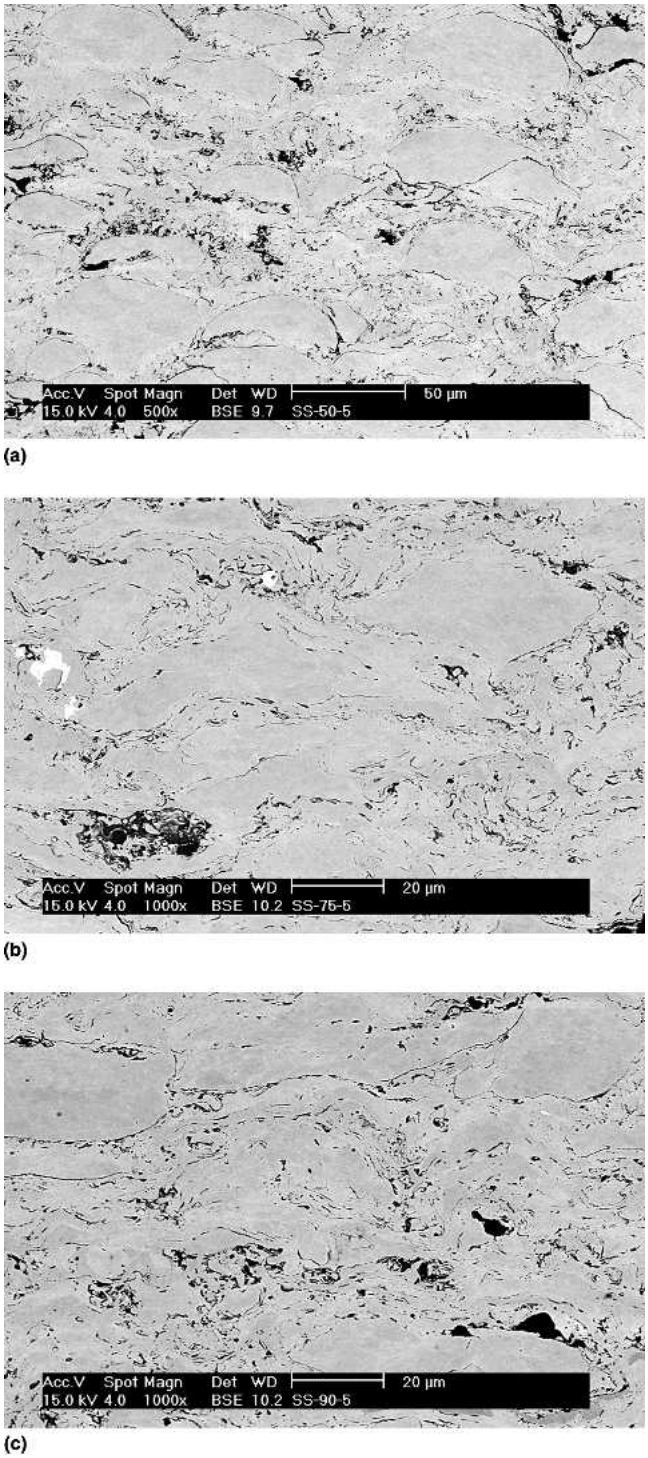

Fig. 1 Microstructure of HVOF 316L SS coatings sprayed at (a) 520 m/s, (b) 610 m/s, and (c) 640 m/s

3. Results

Typical microstructures of coatings formed at the three spray pressures are shown in Fig. 1; quantified microstructural characteristics are listed in Table 2. Coatings sprayed at all velocities show structures typical of HVOF with very little porosity (less than 1%). The fractions of oxide and unmelted particles range from 4.2 to 6.5% for oxide and 20 to 40% for unmelts. In all cases the coatings show relatively high dislocation densities, more than two orders of magnitude greater than the starting powder.

Mechanical characteristics of the coatings are presented in Table 3, along with typical values for annealed, wrought 316 SS.

The as-sprayed coating hardnesses are high, ranging from 31 to 45 HRC and 360-490 VHN. The yield strength, σ_0, was estimated from microhardness using the formula (Ref 22):

$$\sigma_0 = \frac{\text{VHN}}{3}(0.1)^n \quad \text{(Eq 1)}$$

and assuming a work-hardening coefficient, n, of 0.15 [typical of work-hardened metals (Ref 23)]. Again, the values are much higher than those for wrought 316 SS. The coating hardness increases with increasing spray velocity, as observed previously for HVOF Fe_3Al coatings (Ref 20). Annealing at 1000 °C significantly decreases the coating hardness, although not to the level of annealed, wrought 316 SS. The elastic moduli of the coatings (177 and 190 GPa) agree well with that of wrought material (193 GPa).

The thermal expansion behavior of a coating sprayed at 520 m/s is shown in Fig. 2, a plot of mean CTE versus temperature. The expansion data were recorded continuously; the large points only serve to note data from the separate runs. Mean CTE values for wrought 316 SS are shown for comparison. Although the second and third runs show good agreement with wrought behavior, significantly lower expansion is observed for the first run, especially above 550 °C. The lowered CTE in the first run corresponds to a net 0.4% shrinkage of the specimen after cooling to room temperature. No dimensional change was observed after the second and third runs.

Table 2 Microstructural characteristics of HVOF 316L SS coatings

Mean particle velocity, m/s	Porosity V_f, %	Oxide V_f, %	Unmelt V_f, %	Dislocation density, m^{-2}
520	1.1	4.2	40	5.6×10^{14}
610	0.6	6.2	24	7.1×10^{14}
640	0.6	6.5	20	7.0×10^{14}
Starting powder	NM(a)	NM	NM	4.2×10^{12}

(a) NM, not measured

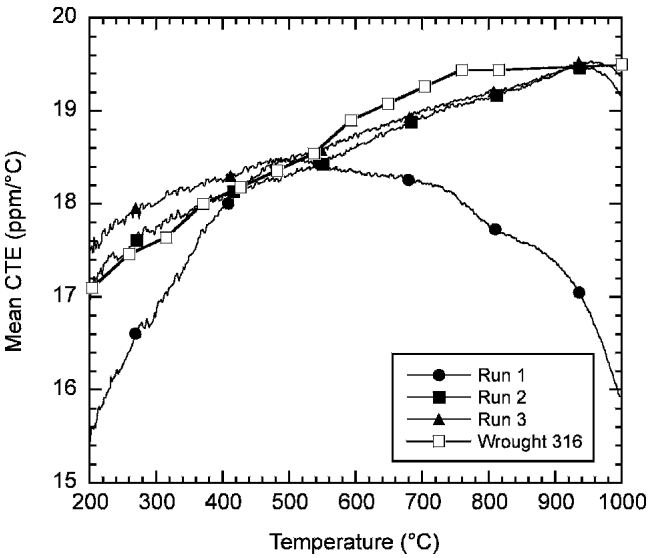

Fig. 2 Thermal expansion coefficient of HVOF 316L SS coatings. Comparative data for wrought 316 SS are from Ref 24.

4. Discussion

The mechanical property differences between the coatings and wrought alloy are readily rationalized in terms of coating microstructure. Because of the strong peening effect imparted by the high-velocity spray particles in the HVOF process, metallic coatings in the as-sprayed condition are usually extremely cold worked with high dislocation densities and hence high hardness. For 316 SS, the estimated yield strengths correspond to the behavior of wrought material cold worked to significantly greater than 60% reduction (Ref 24). Increasing hardness suggests that the peening effect increases with spray particle velocity, although a similarly marked increase is not observed in the dislocation density. Previous studies on Fe_3Al found a more significant increase in dislocation density with particle velocity (Ref 17, 20). Although the high hardness could also be attributed to the oxide content, the size and distribution of the oxide observed suggest otherwise. Oxide is primarily observed along splat boundaries with relatively large particle sizes (>1 μm), which would be ineffective for strengthening. Significant strengthening caused by oxide inclusions in metals requires a very fine, uniform dispersion (Ref 25).

Lau et al. (Ref 11) measured the microhardness of HVOF 316 SS coatings with a nanocrystalline grain structure (the feedstock powders were highly ball milled prior to spraying). Values ranging from 440 to 650 VHN were reported, somewhat higher than the hardness of coatings obtained in the current study using annealed feedstock powders. The authors attribute the high hardness to the nanocrystalline structure imparted by ball milling, but clearly the HVOF process itself makes a significant contribution to hardness.

These results have significant implications for stress modeling of HVOF metallic coatings, especially numerical models which include plasticity. The data show that it is not reasonable to assume that coatings that have not been annealed by high-temperature exposure have the yield strength and work-hardening behavior of wrought material. As shown in Table 2, the hardness of annealed coatings is also significantly greater than equivalent wrought material. The source of the hardness of annealed coatings is currently unknown, but it could be fine grain size or oxide (unresolvable with SEM). Similar behavior was observed for Fe_3Al coatings (Ref 20).

With the exception of thermal expansion in the as-sprayed condition, the physical properties of 316 SS are not altered sig-

Table 3 Mechanical characteristics of HVOF 316L SS coatings and annealed 316 SS

Mean particle velocity, m/s	Elastic modulus, GPa	Macro-hardness	Micro-hardness, VHN_{500}	Corresponding yield strength, MPa
520	177	30.8 HRC	360	830
610	NM(a)	41.9 HRC	430	990
640	190	44.8 HRC	490	1130
640, 1000 °C anneal	NM	NM	230	540
Annealed wrought 316 SS(b)	193	80 HRB	160	240

(a) NM, not measured. (b) Data for 316 SS are taken from Ref 24.

nificantly by the HVOF process. The elastic moduli agree well with wrought values, as does the CTE of the annealed coating (second and third runs). Other researchers have observed significant differences between the physical properties of coatings and wrought materials, even for HVOF spraying (Ref 6, 7). In these cases, however, the differences were associated with significant (>10%) porosity and/or oxide contents in the coating. In the present case, the fractions appear to be sufficiently low so they do not measurably affect physical properties. These results again highlight the potential inaccuracy in assuming or inferring coating properties, which are strongly dependent on the specific coating process.

The low CTE of the as-sprayed coating is attributed to annealing and recrystallization processes occurring during heating to 1000 °C. Similar behavior has been observed for Fe_3Al and FeAl intermetallic coatings (Ref 17, 26). Its observation in a simple solid solution alloy such as 316 SS provides further confirmation that the behavior-low CTE and a small net shrinkage after cooling-primarily results from annealing processes rather than ordering phenomena.

5. Conclusions

- HVOF spraying of type 316 SS coatings resulted in coatings significantly harder than equivalent wrought 316 SS in an annealed condition. The increase is primarily attributed to extensive cold work imparted by high-velocity spray particles.
- The coating elastic modulus agreed well with that for wrought 316 SS.
- A significant decrease in mean CTE was observed for the as-sprayed coating, whereas the thermal expansion of annealed coatings showed good agreement with wrought values. The lowered CTE is attributed to annealing and recrystallization processes occurring during initial heating of the as-sprayed coating.

Acknowledgments

The author acknowledges W.D. Swank and D.C. Haggard for thermal spraying of the coatings and T.C. Morris for metallography. This work was supported by the U.S. Department of Energy, Office of Fossil Energy, under DOE Idaho Operations Office Contract DE-AC07-99ID13727.

References

1. T.W. Clyne and S.C. Gill, Residual Stresses in Thermal Spray Coatings and Their Effect on Interfacial Adhesion: A Review of Recent Work, *J. Thermal Spray Technol.,* Vol 5 (No. 4), 1996, p 401-418
2. S.C. Gill and T.W. Clyne, Stress Distributions and Material Response in Thermal Spraying of Metallic and Ceramic Deposits, *Metallurg. Trans.,* Vol 21B, 1990, p 377-385
3. D.J. Greving, E.F. Rybicki, and J.R. Shadley, Through-Thickness Residual Stress Evaluations for Several Industrial Thermal Spray Coatings Using a Modified Layer Removal Method, *J. Thermal Spray Technol.,* Vol 3 (No. 4), 1994, p 379-388
4. Y.C. Tsui and T.W. Clyne, An Analytical Model for Predicting Residual Stresses in Progressively Deposited Coatings, *Thin Solid Films,* Vol 306, 1997, p 23-33
5. J.S. Wallace and J. Ilavsky, Elastic Modulus Measurements in Plasma-Sprayed Deposits, *J. Thermal Spray Technol.,* Vol 7 (No. 4), 1998, p 521-526
6. J. Dubsky, B. Kolman, P. Ctibor, F. Kroupa, and J. Ilavsky, Structure and Residual Stresses in Thermally Sprayed Coatings, *Functionally Graded Materials,* W.A. Kaysser, Ed., Trans Tech Publications, Ltd., 1998, p 232-237
7. H. Gassot, T. Junquera, V. Ji, M. Jeandin, V. Guipont, C. Coddet, C. Verdy, and L. Grandsire, Comparative Study of Mechanical Properties and Residual Stress Distributions of Copper Coatings Obtained by Different Thermal Spray Processes, *Surface Eng.,* Vol 17 (No. 4), 2001, p 317-322
8. S. Kuroda, Properties and Characterization of Thermal Sprayed Coatings: A Review of Recent Research Progress, *Thermal Spray: Meeting the Challenges of the 21st Century,* C. Coddet, Ed., May 25-29, 1998 (Nice, France), ASM International, 1998, p 539-550
9. E.F. Rybicki, J.R. Shadley, X. Xiong, and D.J. Greving, A Cantilever Beam Method for Evaluating Young's Modulus and Poisson's Ratio of Thermal Spray Coatings, *J. Thermal Spray Technol.,* Vol 4 (No. 4), 1995, p 377-384
10. D. Schwingel, R. Taylor, T. Haubold, J. Wigren, C. Gualco, F. Ladru, E. Lugscheider, and V. Gourlaouen, Thermophysical and Mechanical Properties of PYZ Thick Thermal Barrier Coatings, *Thermal Spray: Meeting the Challenges of the 21st Century,* C. Coddet, Ed., May 25-29, 1998 (Nice, France), ASM International, 1998, p 623-628
11. M.L. Lau, H.G. Jiang, and E.J. Lavernia, Synthesis and Characterization of Nanocrystalline 316-Stainless Steel Coatings by High Velocity Oxy-Fuel Spraying, *Thermal Spray: Meeting the Challenges of the 21st Century,* C. Coddet, Ed., May 25-29, 1998 (Nice, France), ASM International, 1998, p 379-384
12. D. Zhang, S.J. Harris, and D.G. McCartney, Mechanical Properties and Microstructure of HVOF-Sprayed Co and Ni Alloy Coatings, *Thermal Spray 2003: Advancing and Science and Applying the Technology,* C. Moreau and B. Marple, Ed., May 5-8, 2003 (Orlando, FL), ASM International, 2003, p 820-836
13. B. Zha, H. Wang, and X. Su, Structure and Property of Wc-17co Coatings Sprayed by HVO/Af, *Thermal Spray 2003: Advancing the Science and Applying the Technology,* C. Moreau and B. Marple, Ed., May 5-8, 2003 (Orlando, FL), ASM International, 2003, p 837-839
14. T.C. Hanson and G.S. Settles, Particle Temperature and Velocity Effects on the Porosity and Oxidation of an HVOF Corrosion-Control Coating, *J. Thermal Spray Technol.,* Vol 12 (No. 3), 2003, p 403-415
15. O.C. Brandt, Mechanical Properties of HVOF Coatings, *J. Thermal Spray Technol.,* Vol 4 (No. 2), 1995, p 147-152
16. Y. Itoh, M. Saitoh, and M. Tamura, Characteristics of MCrAlY Coatings Sprayed by High-Velocity Oxygen-Fuel Spraying System, *J. Eng. Gas Turbines Power,* Vol 122 (No. 1), 2000, p 43-49
17. T.C. Totemeier, R.N. Wright, and W.D. Swank, Mechanical and Physical Properties of HVOF-Sprayed Iron Aluminide Coatings, *Metallurg. Mater. Trans.,* Vol 34A (No. 10), 2003, p 2223-2231
18. W.D. Swank, J.R. Fincke, D.C. Haggard, and G. Irons, HVOF Gas Flow Field Characteristics, *Thermal Spray Industrial Applications,* C.C. Berndt and S. Sampath, Ed., June 20-24, 1994 (Boston, MA), ASM International, 1994, p 307-312
19. W.D. Swank, J.R. Fincke, D.C. Haggard, G. Irons, and R. Bullock, HVOF Particle Flow Field Characteristics, *Thermal Spray Industrial Applications,* C.C. Berndt and S. Sampath, Ed., June 20-24, 1994 (Boston, MA), ASM International, 1994, p 319-324
20. T.C. Totemeier, R.N. Wright, and W.D. Swank, Microstructure and Stresses in HVOF-Sprayed Iron Aluminide Coatings, *J. Thermal Spray Technol.,* Vol 11 (No. 3), 2002, p 400-408
21. G.K. Williamson and R.E. Smallman, Dislocation Densities in Some Annealed and Cold-Worked Metals from Measurements on the X-Ray Debye-Scherrer Spectrum, *Phil. Mag.,* Vol 1, 1956, p 34
22. J.R. Cahoon, W.H. Broughton, and A.R. Kutzak, The Determination of Yield Strength from Hardness Measurements, *Metallurg. Trans. A,* Vol 2 (No. 7), 1971, p 1979-1983
23. G.E. Dieter, *Mechanical Metallurgy,* 3rd ed., McGraw-Hill, 1986, p 327-332
24. D. Peckner and I.M. Bernstein, *Handbook of Stainless Steels,* McGraw-Hill, New York, 1977, p 20-29
25. J.K. Tien and E.G. Jacobs, Structure of Oxide Dispersion-Strengthened Alloys, *Mechanical Properties of Metallic Composites,* S. Ochiai, Ed., Marcel Dekker, 1994, p 25-40
26. T.C. Totemeier, R.N. Wright, and W.D. Swank, FeAl and Mo-Si-B Intermetallic Coatings Prepared by Thermal Spraying, *Proc. 17th Annual Conference on Fossil Energy Materials,* National Energy Technology Laboratory, Pittsburgh, PA, 2003, available at www.netl.doe.gov